


Analytical Methods for High-Rate Global Quantum Networks

Cillian Harney^{✉*} and Stefano Pirandola[†]

Department of Computer Science, University of York, York YO10 5GH, United Kingdom

 (Received 3 June 2021; revised 18 January 2022; accepted 22 February 2022; published 25 March 2022)

The development of a future global quantum communication network (or quantum Internet) will enable high-rate private communication and entanglement distribution over very long distances. However, the large-scale performance of ground-based quantum networks (which employ photons as information carriers through optical fibers) is fundamentally limited by fiber quality and link length, with the latter being a primary design factor for practical network architectures. While these fundamental limits are well established for arbitrary network topologies, the question of how to best design global architectures remains open. In this work, we introduce a large-scale quantum network model called weakly regular architectures. Such networks are capable of idealizing network connectivity, provide freedom to capture a broad class of spatial topologies, and remain analytically treatable. This allows us to investigate the effectiveness of large-scale networks with consistent connective properties and unveil critical conditions under which end-to-end rates remain optimal. Furthermore, through a strict performance comparison of ideal ground-based quantum networks with that of realistic satellite quantum communication protocols, we establish conditions for which satellites can be used to outperform fiber-based quantum infrastructure, rigorously proving the efficacy of satellite-based technologies for global quantum communications.

DOI: [10.1103/PRXQuantum.3.010349](https://doi.org/10.1103/PRXQuantum.3.010349)

I. INTRODUCTION

Advancements in quantum information science will have a profound impact on society [1–4]. In particular, the overarching trajectory of quantum communication technologies is toward a global quantum communication network: a quantum Internet [5–8]. This will facilitate high-rate provably secure communication and globally distributed quantum information processing, with radical implications for science, technology, and beyond.

The current, most promising, point-to-point quantum communication protocols (where two parties are connected directly via a quantum channel) are based on continuous-variable (CV) quantum systems [9–12] (such as bosonic modes). CV protocols achieve high performance and are compatible with current telecommunication infrastructure based upon optical-fiber connections, emphasizing their near-term feasibility. However, the laws of quantum mechanics prohibit the ability to simultaneously achieve high rates and long distances, a fundamental law captured by the Pirandola-Laurenza-Ottaviani-Banchi

(PLOB) bound [13]. This describes the absolute maximum rate at which two parties may transfer quantum states, distribute entanglement, or establish secret keys over a bosonic lossy channel (optical fibers) equal to $-\log_2(1 - \eta)$ bits per channel use, where η is the channel transmissivity [13,14].

Overcoming this point-to-point limitation requires the use of quantum repeaters or, more generally, the construction of quantum networks. Combining tools from classical network theory [15–18] with the PLOB bound, ultimate limits have also been established for the end-to-end capacities of quantum networks [19]. These results confirm that the PLOB bound can be beaten via quantum networking, facilitating high-rate communication at longer ranges. While such bounds are easily expressed in full generality for arbitrary network topologies, their practical assessment requires the specification of an architecture. Questions of network topology have been recently considered via the statistical study of complex random quantum networks [20–23], which reveal insightful phenomena associated with large-scale network properties. Studies of this kind are extremely valuable and help to unveil important guidelines for the development of future quantum networks.

Nonetheless, such analyses are not easy and require significant numerical effort in order to reveal key network properties, e.g., critical network densities or maximum fiber lengths. There is a demand for versatile *analytical* tools that allow for the efficient benchmarking of quantum

*cth528@york.ac.uk

†stefano.pirandola@york.ac.uk

Published by the American Physical Society under the terms of the [Creative Commons Attribution 4.0 International](https://creativecommons.org/licenses/by/4.0/) license. Further distribution of this work must maintain attribution to the author(s) and the published article's title, journal citation, and DOI.

networks and can motivate the construction of large-scale topologies.

Meanwhile, ground-based fiber channels are not the only conduits available for global quantum communications. A rival infrastructure that may prove superior to fiber-based networks at global distances is satellite quantum communication (SQC) [24–31]. SQC exploits ground-to-satellite communication channels to overcome the fundamental distance limitations offered by fiber- and/or ground-based mechanisms. A satellite in orbit around the Earth may act as a *dynamic* repeater that physically passes over ground-based users and distributes very-long-range entanglement and/or secret keys. The ability to exploit a free-space connection with a satellite also carries the possibility of substantially more transmissive channels than optical fiber, making it ideal for global communication protocols.

The following critical questions emerge. Can we develop analytical tools that allow us to place limits on the end-to-end performance of large-scale quantum networks? And are fiber-based networks truly the best way to achieve long-distance quantum communication? The goal of this work is to make progress with these challenges.

Utilizing ideas from quantum information theory, classical networks, and graph theory [32], we investigate ideal architectures based on the property of weak regularity. Weakly regular networks (WRNs) simultaneously (i) idealize network connectivity, (ii) provide sufficient freedom to capture a broad class of spatial topologies, and (iii) remain analytically treatable so that critical network properties can be rigorously studied. This results in a design with desirable qualities that can efficiently and effectively provide insight for realistic structures. We show that quantum WRNs employing multipath routing admit remarkably accessible and achievable upper bounds on the end-to-end network capacity. This allows for a characterization of the ideal performance of a fiber-based quantum Internet with respect to essential properties such as maximum channel length and nodal density.

Our exact analytical results provide an immediate pathway to perform comparisons of SQC with global ground-based quantum communications. We study the average number of secret bits per day that can be distributed between two remote stations, using large-scale quantum fiber networks or a single-satellite repeater station in orbit. Our findings rigorously prove the superiority of satellite-based quantum repeaters for global quantum communications, revealing the constraints associated with fiber-based networks and the enormous resource demands required to overcome achievable rates offered by a single satellite. These results further motivate the study of SQC and its key role within a future quantum Internet.

The remainder of this paper is structured as follows. In Sec. II, we introduce preliminary notions of quantum networks, optimal end-to-end performance, and ideal

properties of large-scale network designs. In Sec. III, we discuss how the optimal performance of quantum WRNs can be analytically bounded with respect to network properties and apply these methods to bosonic lossy networks. Section IV then compares the performance of global fiber networks with rates that are achievable by SQC, assessing the advantages associated with each infrastructure, followed by concluding remarks in Sec. V.

II. QUANTUM NETWORK DESIGN

A. Basics of quantum networks

A quantum network can be described as a finite undirected graph $\mathcal{N} = (P, E)$, where $P = \{\mathbf{x}_i\}_i$ is a set of all nodes on the graph and $E = \{e_i\}_i$ collects valid connections between pairs of nodes (edges). A network node refers to either a user node, such as a potential end-user pair Alice \mathbf{a} and Bob \mathbf{b} , or a repeater or relay node. Each node \mathbf{x}_i possesses a local register of quantum systems that can be altered and exchanged with connected neighbors. Any two nodes $\mathbf{x}, \mathbf{y} \in P$ are connected via an undirected edge $e := (\mathbf{x}, \mathbf{y}) \in E$ if there exists a quantum channel $\mathcal{E}_{\mathbf{x}\mathbf{y}}$ through which they may directly communicate. Since each edge is undirected, this may be a forward or backward channel.

In the context of quantum networks, it is important to make a distinction between *physical flow* and *logical flow*. The logical flow of a quantum communication channel describes the direction in which entanglement, secret keys, or quantum states are distributed from a node \mathbf{x} to node \mathbf{y} (or vice versa). The physical flow of quantum communication refers to the actual direction of quantum system exchange, i.e., if quantum systems are physically sent in the direction $\mathbf{x} \rightarrow \mathbf{y}$ or $\mathbf{y} \rightarrow \mathbf{x}$. In a quantum network, these concepts can be completely decoupled. This may be due to the fact that the communication task has a symmetric objective, i.e., if Alice and Bob wish to share a secret key, they do not care *who* initiates the exchange of quantum systems. However, it may also be due to quantum teleportation; it is always possible to “reverse” the logical direction of communication by means of a teleportation protocol between Alice and Bob.

The independence of physical and logical flow helps us to reliably describe a quantum network as an undirected graph. Any pair of connected network nodes can choose the physical direction in which they wish to exchange quantum systems and may always choose that which has the largest capacity. As a result, we never need to distinguish between forward or backward channels and we represent each edge $(\mathbf{x}, \mathbf{y}) \in E$ by the best choice of quantum channel [19].

In a point-to-point communication setting, the logical flow of quantum information has a clear and obvious set of choices; Alice to Bob $\mathbf{a} \rightarrow \mathbf{b}$ or Bob to Alice $\mathbf{a} \leftarrow \mathbf{b}$. However, within a quantum network, a vast array of options

emerge due to the various interconnections and possible paths that information may follow. To address this, users can devise an end-to-end routing strategy that facilitates communication between end users. The two key classes of strategy are *single-path* and *multipath* routing.

Single-path routing is the simplest network communication method, which utilizes point-to-point communications in a sequential manner. An end-to-end route, ω , is defined as a sequence of network edges that are able to connect a pair of end users $\mathbf{a}, \mathbf{b} \in P$, that is, $\omega := \{(\mathbf{a}, \mathbf{x}_1), (\mathbf{x}_1, \mathbf{x}_2), \dots, (\mathbf{x}_N, \mathbf{b})\}$. Quantum systems can be exchanged from node to node along this route, followed by local operations assisted by classical communication (LOCCs) after each transmission, until eventually communication is established between the end users. This kind of strategy is analogous to the use of a repeater chain and network performance is determined by the strength of each link along an optimal end-to-end route. Yet, quantum information is significantly less robust than classical information and single-path routing may not be sufficiently resilient to network errors or provide high enough rates.

A more powerful strategy is multipath routing, which properly exploits the multitude of possible end-to-end routes available in a quantum network. In multipath protocols, users may simultaneously utilize a number of unique routes $\{\omega_1, \omega_2, \dots, \omega_M\}$ in an effort to enhance their end-to-end rate. A user may exchange an initially multipartite quantum state with a number of neighboring receiver nodes, who may each then perform their own point-to-multipoint exchanges along its unused edges. The exchange of quantum systems can be interleaved with adaptive network LOCCs in order to distribute secret correlations and this process continues until a multipoint interaction is carried out with the end user.

The optimal multipath routing strategy operates in such a way that all channels in the network are used once per end-to-end transmission. This is known as a *flooding protocol* [17–19]; each node in the network performs quantum systems exchanges along all its available edges, resulting in nonoverlapping point-to-multipoint exchanges between all network nodes. The ability to flood an entire network means that every possible end-to-end route between the end users is fully explored, allowing them to achieve the optimal end-to-end rate. This greatly enhances the end-to-end performance of quantum networks.

B. Optimal performance and flooding capacities

As discussed, the optimal end-to-end performance of a network is defined by its ability to perform flooding by using every edge in the network to achieve communication between a pair of end users [19]. Any communication protocol that does not flood the network utilizes fewer resources and thus fewer end-to-end paths; hence no protocol can achieve a better end-to-end rate than flooding. This

optimal performance is quantified by a *flooding capacity* $C^m(\mathbf{i}, \mathcal{N})$, which describes the optimal number of target bits (such as secret bits or entanglement bits) that can be transmitted between end users per use of a flooding protocol.

An important graph-theoretic concept for quantifying network performance is that of *cuts* and *cut sets*. Consider a network $\mathcal{N} = (P, E)$ with two remote end users $\mathbf{a}, \mathbf{b} \in P$. We may collect this end-user pair into its own, compact object $\mathbf{i} = \{\mathbf{a}, \mathbf{b}\}$, which is simply a two-element subset of the collection of all network nodes. We define a cut C as a bipartition of all network nodes P into two disjoint subsets of nodes (P_a, P_b) such that the end users become completely disconnected; $\mathbf{a} \in P_a$ and $\mathbf{b} \in P_b$, where $P_a \cap P_b = \emptyset$. A cut C generates an associated cut set; a collection of network edges \tilde{C} that enforce the partitioning when removed,

$$\tilde{C} := \{(\mathbf{x}, \mathbf{y}) \in E \mid \mathbf{a} \in P_a, \mathbf{b} \in P_b\}. \quad (1)$$

Under the action of a cut, a network is successfully partitioned,

$$\mathcal{N} = (P, E) \xrightarrow{\text{Cut: } C} (P, E \setminus \tilde{C}) = (P_a \cup P_b, E \setminus \tilde{C}), \quad (2)$$

so that there no longer exists a path between \mathbf{a} and \mathbf{b} . Network cuts play a key role in the derivation of end-to-end network rates and many network-optimization tasks can be reduced to an optimization over all cuts with respect to single-edge or multiedge properties.

Each channel in a network is associated with a single-edge capacity $C_{xy} := \mathcal{C}(\mathcal{E}_{xy})$, which describes the point-to-point communication quality between nodes. Hence, all networks have a single-edge capacity distribution $\{C_{xy}\}_{(\mathbf{x}, \mathbf{y}) \in E}$, which informs the weights of the network graph. Consequently, the flooding capacity can be derived by solving the classical maximum-flow minimum-cut problem according to a single-edge capacity distribution. The flooding capacity is found by locating the minimum cut, C_{\min} , that minimizes the multiedge capacity over all cut sets [19]:

$$C^m(\mathbf{i}, \mathcal{N}) := \min_C \sum_{(\mathbf{x}, \mathbf{y}) \in \tilde{C}} C_{xy}. \quad (3)$$

For general quantum networks with arbitrary capacity distributions and network structures, this problem requires a numerical treatment by solving the well-known max-flow min-cut problem [33–35] to find C_{\min} . However, it is possible to express an intuitive simpler upper bound. Let us define the nodal neighborhood of a node \mathbf{x} as

$$N_x := \{\mathbf{y} \mid (\mathbf{x}, \mathbf{y}) \in E\}. \quad (4)$$

Then, N_x is the collection of nodes to which \mathbf{x} is connected. We can also define an edge neighborhood of \mathbf{x} as all the

edges that connect \mathbf{x} to its neighbors:

$$E_{\mathbf{x}} := \{(\mathbf{x}, \mathbf{y}) | \mathbf{y} \in N_{\mathbf{x}}\}. \quad (5)$$

It follows that one can always successfully partition the users \mathbf{a} and \mathbf{b} by collecting all of the edges in $E_{\mathbf{a}}$ or $E_{\mathbf{b}}$ into a cut set. This effectively disconnects either of the nodes from the rest of the network, resulting in a valid cut, and is true regardless of the network architecture. We may call this form of network cut *user-node isolation*, denoted by C_{iso} .

Since this form of cut always exists, the multiedge capacity associated with C_{iso} can be used to upper bound Eq. (3). By performing nodal isolation on the end user in $\mathbf{i} = \{\mathbf{a}, \mathbf{b}\}$ that minimizes its multiedge capacity, we can write the bound

$$C^m(\mathbf{i}, \mathcal{N}) \leq C_{\mathcal{N}_i}^m := \min_{\mathbf{j} \in \mathbf{i}} \sum_{(\mathbf{x}, \mathbf{y}) \in E_{\mathbf{j}}} C_{\mathbf{xy}}. \quad (6)$$

Here, we define $C_{\mathcal{N}_i}^m$ as the *min-neighborhood capacity*, which is generated by C_{iso} . Since C_{iso} is a valid network cut, the min-neighborhood capacity is achievable.

C. Ideal properties of large-scale networks

An overarching goal of quantum network design is to achieve *end-to-end-distance independence*: that is, given a pair of end users, the rate achievable between them is independent from their physical end-to-end separation and instead encoded into some properties of network link lengths or nodal density. In quantum networks, distance independence is especially important as it bypasses the fundamental rate limitations associated with point-to-point communications imposed by the PLOB bound. Recent studies have shown that random fiber-network architectures that are explicitly conscious of link lengths are capable of obtaining distance independence; e.g., Waxman networks, which are sufficiently dense [22,36]. These studies simultaneously suggest the shortcomings of classically inspired network architectures (such as scale-free structures) to achieve distance independence in a quantum setting, even with large resources.

It is imperative that quantum networks are constructed using quantum motivated design choices. To facilitate end-to-end-distance independence, ground-based quantum network architectures will need to be especially conscious of two main features; maximum link length (which is often encoded into nodal density) and network connectivity (how well connected each node is within the structure). When appropriate restrictions are placed on permitted link lengths, this can help to ensure strong end-to-end rates. Until now, investigations of the relationship between large-scale quantum network properties and performance have been excluded to numerical studies. For example, in Refs. [21,22], the authors study the necessary nodal

densities required to ensure effective end-to-end rates; the higher the network density, the more likely it is that end-to-end communication can be mediated by shorter links, resulting in reliable rates. In this work, we reveal novel analytical tools that help to uncover the necessary resources for high-performance quantum fiber networks.

III. WEAKLY REGULAR QUANTUM NETWORKS

A. Weakly regular networks

The generality of complex architectures such as Waxman, Erdős-Rényi, and scale-free networks renders analytical investigation very difficult. For this reason, the investigation of quantum repeater technologies and protocols often relies heavily on numerics in order to study complex network performance. Otherwise, one is limited to the simpler setting of linear networks that can be assessed analytically, i.e., repeater chains. The development of a common ground between these scenarios, where large-scale highly connected networks can be studied analytically, is thus highly desirable.

Here, we propose the use of *weakly regular* (WR) network architectures. Weak regularity is a graph-theoretic concept that confers particular connectivity properties onto undirected graphs, $\mathcal{N} = (P, E)$. Most prominently, each node $\mathbf{x} \in P$ in a WRN has the same degree, i.e., if $\mathbf{x} \in P$ is connected to k other nodes, then every node in the network is connected to exactly k nodes. This infers *regularity* and provides the core simplification from complex graphical designs (where regularity is seldom held).

The *weak* element of weak regularity is less obvious but is similarly integral to our analyses. By definition, a *strongly regular* graph is a structure that adheres to very strict rules; it consists of n nodes that are all k regular; any pair of adjacent nodes (nodes that share an edge) shares exactly λ common neighbors and any pair of nonadjacent nodes (do not share an edge) shares exactly μ neighbors. We call these positive integer parameters $\lambda, \mu \in \mathbb{Z}^+$ the adjacent and nonadjacent commonalities, respectively, of any two nodes on the graph and they are used to characterize how a graph is connected. The notion of strength in strong regularity resides in the consistency of the values λ and μ for all nodes across the graph. When strong regularity is upheld, all of these requests result in a relatively small graph with impractical properties for large-scale network design. Consequently, if λ and μ are allowed to take on a broader range of values, then the graph is *weakly* regular. Hence, weakness infers a looser characterization of neighbor sharing between nodes.

In this work, we consider WR graphs for which the neighbor-sharing (commonality) properties of any network node can obey some *spectrum* of values. In the context of studying end-to-end performance, it turns out that the most important commonality property is the adjacent commonality. Consider a node $\mathbf{x} \in P$ on a k -WR graph and its

neighborhood of adjacent nodes,

$$N_{\mathbf{x}} := \{\mathbf{y} | (\mathbf{x}, \mathbf{y}) \in E\}. \quad (7)$$

Then, $N_{\mathbf{x}}$ is the collection of k nodes to which \mathbf{x} is connected. For any node on the network, we can define a bespoke *adjacent-commonality multiset* (a modified set that can contain degenerate elements), which counts the number of neighbors shared between \mathbf{x} and all its neighbors $\mathbf{y} \in N_{\mathbf{x}}$. More precisely, the adjacent-commonality multiset can be defined as

$$\lambda_{\mathbf{x}} := \{|N_{\mathbf{x}} \cap N_{\mathbf{y}}| \mid (\mathbf{x}, \mathbf{y}) \in E\} = \{\lambda_{\mathbf{x}}^{\mathbf{y}}\}_{\mathbf{y} \in N_{\mathbf{x}}}, \quad (8)$$

where we denote $\lambda_{\mathbf{x}}^{\mathbf{y}} := |N_{\mathbf{x}} \cap N_{\mathbf{y}}|$ as the number of common neighbors shared between the connected nodes \mathbf{x} and \mathbf{y} . In our analyses, we consider graphs that are defined by a nondegenerate superset of permitted adjacent-commonality multisets,

$$\Lambda := \{\lambda_{\mathbf{x}} | \mathbf{x} \in P\}, \quad (9)$$

so that the adjacent-commonality multiset of any node in the network $\mathbf{x} \in P$ belongs to the set $\lambda_{\mathbf{x}} \in \Lambda$.

In summary, we are able to define a (k, Λ) WRN as a class of network for which all nodes have a constant degree equal to k and for which their neighbor-sharing properties satisfy $\lambda_{\mathbf{x}} \in \Lambda$. While k and Λ impose connectivity constraints, WRNs that belong to this class are free to adopt a vast range of topological or spatial configurations. Furthermore, we avoid explicit references to the number of network nodes n . Instead, n is encoded into properties of

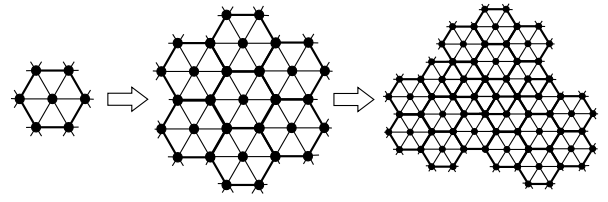


FIG. 1. A WRN cell can be concatenated many times to construct a large-scale network that is WR within some nodal boundary. Alternatively, outer edges can be looped in order to close the network so as to satisfy weak regularity everywhere (so there is no nodal boundary). In this example, $k = 6$ and there is only one unique adjacent-commonality multiset $\lambda = \{2\}^{\cup 6}$ (we employ a superscript union notation to describe the repeated union of a single set, e.g., $\{x\}^{\cup 3} = \{x\} \cup \{x\} \cup \{x\} = \{x, x, x\}$).

the network such as the nodal density $\rho_{\mathcal{N}}$, which defines the average number of network nodes per unit of area.

While these definitions may seem overly abstract, they introduce a remarkably versatile way to analytically describe interesting and useful network structures. For example, it is easy to construct a WR *network cell*; a collection of nodes connected a particular graphical structure, which when concatenated (or “stitched”) together will result in a large-scale network that obeys weak regularity within some nodal boundary. This permits the analytical investigation of networks consisting of many nodes that display highly connected, yet realistic, properties. This concatenation process is visualized in Fig. 1, where it is shown how a $k = 6$ regular cell can be used to generate a larger WRN. Furthermore, Fig. 2(a) depicts a number of examples of these network cells. For more precise details and discussions, see the Supplemental Material [37].

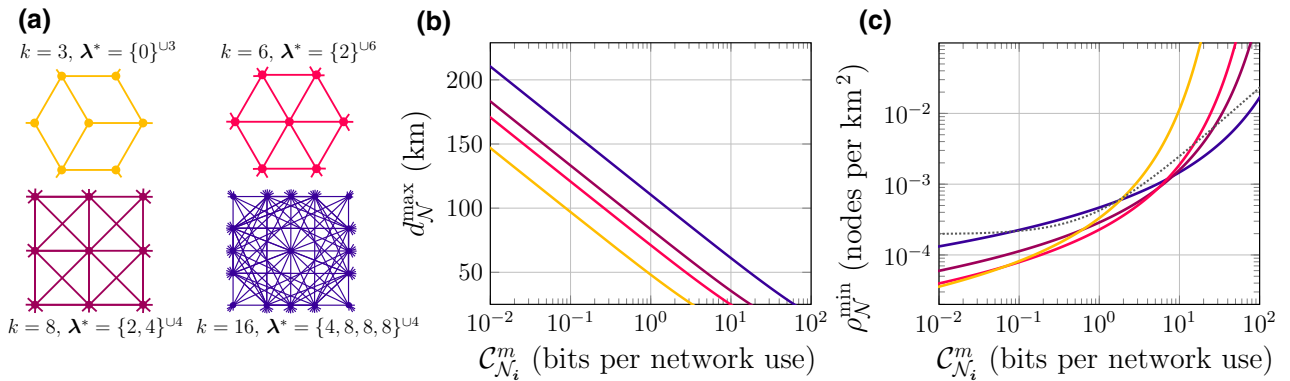


FIG. 2. (a) Examples of network cells that can be used to construct quantum WRNs, where k denotes regularity and λ^* is the adjacent-commonality multiset that minimizes the quantity in Eq. (11). These quantities characterize the network cell and larger WRNs that they can construct. (b) The relationship between the optimal end-to-end flooding capacity (equal to the min-neighborhood capacity $C_{\mathcal{N}_i}^m$) and the maximum link length $d_{\mathcal{N}}^{\max}$ required to guarantee it for bosonic lossy quantum networks according to Eq. (12). The plots are color coordinated with the network cells. Greater network regularity leads to larger permissible ranges of channel lengths. (c) This relationship is depicted between minimum nodal density $\rho_{\mathcal{N}}^{\min}$ with respect to optimal performance for bosonic lossy quantum networks, color coordinated with the network cells. The gray dotted line relates the nodal density to the average flooding capacity between any pair of nodes in a Waxman network, as in Eq. (18) [22].

B. Optimal performance of weakly regular networks

As a network becomes more highly connected, it becomes easier to locate end-to-end routes between any pair of nodes. As a result, the performance of network cuts requires the collection of more and more edges in a cut set, \tilde{C} , in order to restrict flow along the many potential connective paths between the end users. In a spatial network, this initiates a relationship between the cut-set cardinality, $|\tilde{C}|$, and the distance from an end user. The performance of cuts with edges further away from a user node requires the collection of many more edges to consolidate the partition. The further from the user nodes we begin the cut, the greater is the number of potential end-to-end paths we must restrict (since we permit a larger flow from the user node) and thus the more edges we must collect. We call this phenomenon *network-cut growth*.

When the quality of point-to-point links in a network is consistent (link lengths are close to the overall average), then cut-set cardinality $|\tilde{C}|$ plays a significant role in the characterization of minimum cuts. Indeed, for dense networks with distance-constrained edges, the minimum cut is often achieved by nodal isolation. This is due to network-cut growth and consistent single-edge rates; cuts performed further away from the user node will generate a larger multiedge capacity, since they will reliably contain more edges with similar single-edge rates. This kind of behavior has been observed with respect to multipath capacities in Waxman networks and may exist in other very popular random-network models [22,36]. This form of network-cut behavior is indicative of a well-connected network and one that will achieve high rates.

This logic motivates the main theoretical tool utilized in this paper. WRNs also undergo network-cut growth with respect to distance from end users, due to their reliable and consistent connective properties. Consider a large-scale (k, Λ) -WR quantum fiber network and a pair of end users $\mathbf{i} = \{\mathbf{a}, \mathbf{b}\}$ located within it. Then, the cut that collects the fewest edges is that which performs user-node isolation, i.e., collects the k neighboring edges of either end user, generating $\mathcal{C}_{\mathcal{N}_i}^m$ defined in Eq. (6). Every other cut in the network will necessarily collect more than k edges in order to successfully partition the end users. When the flooding capacity saturates Eq. (6), it is user-node isolation that achieves the minimum cut.

Unlike more complex random-network models, it is possible to analytically study network-cut growth within WRNs. Here, we sketch the basic technique and point the reader toward more sophisticated precise arguments in the Supplemental Material [37]. The basic idea is to use the quantities k and Λ to determine how much larger a cut set will grow when one is not permitted to cut user-neighborhood edges. If we know how much a cut set will grow in size with respect to distance from an end-user node, we can identify a relationship between cut-set

cardinality and the link quality requirements necessary to achieve the minimum cut. Ultimately, this helps us to derive a *minimum single-edge threshold capacity* \mathcal{C}_{\min} . This reveals a minimum link quality that, when imposed upon all edges in the network, will ensure that the optimal performance between end users is guaranteed to be equal to the min-user neighborhood capacity, $\mathcal{C}^m(\mathbf{i}, \mathcal{N}) = \mathcal{C}_{\mathcal{N}_i}^m$.

This technique proves to be powerful and versatile. Indeed, given the quantum channel description of single edges in the network, \mathcal{C}_{\min} can be used to relate threshold properties of point-to-point quantum channels and end-to-end performance. In the following, we employ this technique to reveal maximum link lengths for quantum networks connected by bosonic lossy channels.

C. Bosonic lossy quantum networks

When considering fiber-based networks, point-to-point links are described by bosonic pure-loss (lossy) channels. A lossy channel \mathcal{L} with transmissivity $\eta \in (0, 1)$ is a phase-insensitive Gaussian quantum channel, which transforms input quadratures $\hat{\mathbf{x}} = (\hat{q}, \hat{p})^T$ according to $\hat{\mathbf{x}} \mapsto \sqrt{\eta}\hat{\mathbf{x}} + \sqrt{1-\eta}\hat{\mathbf{x}}_{\text{env}}$ (where the environment is in a vacuum state) describing the interaction of a bosonic mode with a zero-temperature bath [10].

For lossy quantum networks, the most important property is the channel length or, from a network perspective, the *internodal separation*. For a given edge $(\mathbf{x}, \mathbf{y}) \in E$ connecting two users in a network, the internodal separation is simply the distance $d_{\mathbf{xy}}$ between them. All two-way assisted quantum and private capacities of the lossy channel are precisely known via the PLOB bound [13],

$$\mathcal{C}_{\mathcal{L}}(d_{\mathbf{xy}}) = -\log_2(1 - 10^{-\gamma d_{\mathbf{xy}}}), \quad (10)$$

where the internodal separation is related to the transmissivity via $\eta_{\mathbf{xy}} = 10^{-\gamma d_{\mathbf{xy}}}$. For current state-of-the-art fiber optics, the loss rate is $\gamma = 0.02$ per kilometer (which equates to a loss rate of 0.2 dB/km). Since these separations directly dictate the channel quality between nodes, they must be precisely engineered and distributed in order to guarantee strong end-to-end performance.

For WR bosonic lossy fiber networks, one can use the technique sketched in the previous section to reveal a maximum fiber length allowed within the network to guarantee optimal end-to-end performance. Consider an end-user pair $\mathbf{i} = \{\mathbf{a}, \mathbf{b}\}$ and a desired min-user neighborhood capacity, $\mathcal{C}_{\mathcal{N}_i}^m$. Let us define the quantities δ and ω as

$$\delta := \min_{\lambda \in \Lambda} \sum_{\lambda \in \lambda} (k - \lambda - 1), \quad \omega := \frac{2(k-1)}{\delta}, \quad (11)$$

which are characteristic quantities of any $(k, \mathbf{\Lambda})$ -WR network. Then, there exists a maximum fiber length

$$d_{\mathcal{N}}^{\max} := -\frac{1}{\gamma} \log_{10} \left(1 - 2^{-\frac{1}{\delta} C_{\mathcal{N}_i}^m} \right), \quad (12)$$

for all edges in the network $(\mathbf{x}, \mathbf{y}) \in E$ so that the end-to-end flooding capacity is guaranteed to satisfy

$$\omega C_{\mathcal{N}_i}^m \leq C^m(\mathbf{i}, \mathcal{N}) \leq C_{\mathcal{N}_i}^m. \quad (13)$$

If the maximum link length is not obeyed for all edges, $C_{\mathcal{N}_i}^m$ remains an upper bound on end-to-end performance.

The parameter ω can be considered as a confidence measure on this performance guarantee. It arises out of a very-worst-case scenario in which all edges surrounding the neighborhood of an end user may be of maximum length $d_{\mathcal{N}}^{\max}$. This may compromise the minimum cut, potentially introducing a minor degradation of the flooding rate. Fortunately, ω is typically of order $10^{-1} - 1$, providing tight bounds in Eq. (13). For example, given the WRN cells in Fig. 2(a), we find a worst-case value of $\omega = 15/64 \approx 0.23$ for $k = 16$, while for $k = 3$ it is exactly $\omega = 2/3$.

In general, this worst-case scenario will not be true and the upper bound in Eq. (13) will nearly always be saturated. Nonetheless, it is possible to provide equality by imposing a slightly stricter distance constraint on the network edges connected to end users. That is, by additionally enforcing that any edge $(\mathbf{x}, \mathbf{y}) \in E_{\mathbf{a}} \cup E_{\mathbf{b}}$ is shorter than

$$d_{\mathcal{N}_i}^{\max} := -\frac{1}{\gamma} \log_{10} \left(1 - 2^{-\left(\frac{1}{k-1} - \frac{1}{\delta}\right) C_{\mathcal{N}_i}^m} \right) \leq d_{\mathcal{N}}^{\max}, \quad (14)$$

we can guarantee that the end-to-end flooding capacity satisfies

$$C^m(\mathbf{i}, \mathcal{N}) = C_{\mathcal{N}_i}^m. \quad (15)$$

Throughout our investigation, we focus on this more probable performance guarantee that the end-to-end flooding capacity satisfies $C^m(\mathbf{i}, \mathcal{N}) = C_{\mathcal{N}_i}^m$ granted that Eq. (12) is respected throughout the entire network. This allows us to effectively characterize the true optimal performance for WR quantum fiber networks.

Full details and derivations of these results can be found in the Supplemental Material [37]. Clearly, the quantity δ in Eq. (11) is vital to our developments. Precisely, δ represents the smallest cut-set cardinality that can be achieved without cutting user-connected edges. In more intuitive terms, it is used to monitor the network-cut growth of a WRN and it allows us to derive critical quantities such as the maximum fiber length above. Note that in Fig. 2(a), each of the WR cells are characterized by its regularity k and the adjacent-commonality multiset that achieves the minimization in δ , denoted by λ^* . Figure 2(b) then illustrates the relationship between the flooding capacity and

the maximum fiber length for a number of example WRNs. The limiting separation $d_{\mathcal{N}}^{\max}$ is inexorably linked to the regularity of the WRN; networks with high connectivity possess a greater tolerance for longer-distance channels, since the enhanced multipath capabilities of the network outweigh the effect of poor-quality channels. This is clear from the examples shown in Fig. 2, where a WRN with degree $k = 16$ can tolerate channels approximately 60 km longer than one with $k = 3$.

D. Nodal density

We have discussed how WRNs can be used to describe realistic large-scale networks while maintaining analytical understanding of their optimal end-to-end performance and critical properties, e.g., the maximum link length. We may take this analysis a step further in order to understand the relationship between end-to-end performance and network nodal density. The nodal density is defined as the number of nodes n per unit area A of the network,

$$\rho_{\mathcal{N}} := n/A. \quad (16)$$

Via the previous section, we may derive a maximum fiber length $d_{\mathcal{N}}^{\max}$ that is necessary to guarantee some optimal end-to-end performance $C^m(\mathbf{i}, \mathcal{N}) = C_{\mathcal{N}_i}^m$. We may then ask the question: Is there a corresponding *minimum nodal density* in which the $(k, \mathbf{\Lambda})$ WRN can be constructed while remaining compliant with the maximum fiber length? It is not so easy to answer this question for completely general WR architectures. Nonetheless, for the networks studied in this work, this challenge is readily tackled.

In the Supplemental Material [37], we show that via the concept of sparse constructions (the least dense way to construct a network given connectivity rules and link-length constraints), it is possible to derive a minimum nodal density $\rho_{\mathcal{N}}^{\min}$ required to achieve optimal end-to-end flooding capacity. The consistency of WRN cells in Fig. 2(a) reduces this to a geometric problem that is solvable. In summary, we can find a lower bound on the nodal density required to achieve optimal performance $C^m(\mathbf{i}, \mathcal{N}) = C_{\mathcal{N}_i}^m$, given by

$$\rho_{\mathcal{N}} \geq \rho_{\mathcal{N}}^{\min} := \xi \gamma^2 \left[\log_{10} \left(1 - 2^{-\frac{1}{\delta} C_{\mathcal{N}_i}^m} \right) \right]^{-2}. \quad (17)$$

Here, ξ is a characteristic quantity of the WR network, found by studying its sparse construction. The tightness of this lower bound depends on the manner in which the sparse construction is solved or approximated.

Figure 2(c) depicts the connection between the flooding capacity and the minimum nodal density for a number of types of WRNs. It is clear that there is a trade-off between end-to-end performance and regular nodal degree. At low flooding rates (10^{-2} – 10^{-1} bits per network use), the WR

structures with lower degrees $k = 3$ and 6 demand fewer resources to achieve the same performance as those with higher degrees $k = 8$ and 16. In this regime, high degrees are not necessary everywhere in the network to achieve the flooding rates; indeed, the consistent connectivity invoked by WR designs helps to maintain performance at low densities. Yet, as the flooding capacity transitions toward 1–10 bits per network use, this behavior changes; WRNs with low degrees demand shorter and shorter links to achieve the high rates and the inability to involve more connections at each node becomes costly. As can be seen, for $k = 3$, the required minimum nodal density rapidly increases, shortly followed by $k = 6$ and $k = 8$. On the contrary, the regime of high end-to-end rates is well suited to WRNs with greater regularity, $k = 16$, for which the greater number of connections at each node facilitates a lower overall density.

Simultaneously, we plot an approximation of the average flooding capacity between any pair of nodes on a Waxman network with respect to the nodal density (dashed gray line) as derived in Ref. [22]. This defines an expected flooding capacity between any pair of users, such that

$$\mathbb{E}_i [C^m(\mathbf{i}, \mathcal{N})] \approx \zeta(\rho_{\mathcal{N}} - \rho_{\text{crit}}) + 1, \quad (18)$$

where $\rho_{\text{crit}} \approx 4.25 \times 10^{-4}$, $\zeta \approx 4358$ and the average $\mathbb{E}_i[\cdot]$ is taken over all possible end-user pairs in the network. We identify a kinship between the necessary $\rho_{\mathcal{N}}^{\text{min}}$ predicted by WRNs and that derived for Waxman networks. As one may expect, the order and consistency of WRNs is able to promise lower resource demands at lower rates; resulting in smaller critical-nodal-density predictions for the necessary density to achieve 1 bit per network use. However, as the flooding performance increases, the flexibility of the Waxman design (its ability to utilize variable nodal degrees) renders it superior to the lower-degree WR structures. In summary, there is good behavioral agreement between these models, corroborating the utility of WR structures as a valuable analytical tool for quantum network design.

IV. COMPARISON WITH SATELLITE QUANTUM COMMUNICATIONS

A. Satellite quantum communications

Here, we briefly review key results that facilitate a comparison of SQC with idealized ground-based quantum networks. For more detailed derivations and discussions of these results, see Refs. [24,26].

Consider two users (Alice and Bob), who choose to communicate by means of an orbiting satellite (a dynamic repeater). Here, we consider a ground station G at approximately sea level and a satellite S that is in orbit at an altitude $h \geq 100$ km and variable zenith angle θ . Given that the radius of the Earth is $R_E \approx 6371$ km, the slant distance between G and S is $z(h, \theta) = \sqrt{h^2 + 2hR_E + R_E^2 \cos^2(\theta)} -$

$R_E \cos(\theta)$, describing the true distance that an optical beam must travel from G to or from S . We may consider two unique configurations for information transmission; *uplink*, which refers to when G is the transmitter and S is the receiver; and *downlink*, where the converse is true. Both configurations will identically admit the effects of free-space diffraction (beam-spot-size widening) and atmospheric extinction (caused by molecular and/or aerosol absorption as the beam propagates). However, additional loss and/or noise effects emerge with respect to uplink and downlink protocols, which invokes an asymmetry in their communication performance.

The effects of turbulence (caused by fluctuations in the atmospheric refractive index) and pointing errors (alignment of the optical signal with the receiver) are responsible for beam wandering, which instigates a fading process for the communication channels. For uplink protocols, turbulence is a significant factor for loss properties of the ground-satellite channel, since it impacts the propagating beam immediately after transmission. However, pointing errors can be reduced due to the ability to easily access and optimize adaptive optics at ground level. In downlink, these effects are reversed. Turbulence is not a factor until the beam reaches low altitudes, at which point the beam has already spread via diffraction. Hence turbulence can be neglected for downlink but pointing errors must be considered due to limited onboard access and resources.

Considering each of these physical effects characterizing the lossy free-space channel, it is possible to present an ultimate limit on the secret-key capacity K for SQC [26],

$$K \leq -\Delta(\eta, \sigma) \log_2(1 - \eta). \quad (19)$$

Here, $\Delta(\eta, \sigma)$ is a correction factor to the PLOB bound, where $\eta := \eta(h, \theta)$ is an effective transmissivity, which is a function of the geometric position, encompassing all the effects of diffraction, extinction, and optical imperfections and/or inefficiencies. Meanwhile, $\sigma^2 = \sigma_{\text{turb}}^2 + \sigma_{\text{point}}^2$ is the variance of the Gaussian random walk of the beam centroid caused by beam wandering, with contributions from turbulence and/or pointing errors.

This bound can be further modified to account for the presence of thermal noise, which is highly dependent upon the time of day (daytime or nighttime) and the weather conditions (cloudy or clear skies). For nighttime communications, background noise is practically negligible and the above bound requires little modification. However, for daytime operations, this is generally not the case and the free-space lossy channels must be described as thermal-loss channels that account for additional noise.

B. Practical key rates for satellite quantum communications

The bound in Eq. (19) is an ultimate upper bound on the capacity of a ground-to-satellite communication channel;

it is important to provide an assessment of realistic and practical protocols that embody achievable lower bounds for SQC. These lower bounds will facilitate comparisons with global quantum networks and help deduce the conditions for which we can expect satellite advantage for long-distance quantum communications.

Here, we summarize some achievable rates for different satellite configurations. We consider practical composable secure secret key rates achievable from the pilot-guided and postselected CV-quantum key distribution (QKD) protocol studied in Refs. [24,26]. The main concept of this protocol is to encode information into Gaussian-modulated coherent states, randomly interleaved by highly energetic pilot pulses used to monitor the transmissivity and fading properties of the free-space channel in real time (facilitating the use of classical postselection). This protocol has been comprehensively extended to account for the physical scenario of satellite quantum communications, resulting in realistic and practical rates.

We may consider the employment of such a protocol in conjunction with a near-polar sun-synchronous satellite used to communicate between two ground stations. This type of orbit ensures a consistent flyover time for any point on the Earth's surface, such that the satellite passes over any point at the same local mean solar time each day. This provides the possibility of stable conditions for satellite communications at around the same time each day. Let us assume that the stations lie along the orbital path such that the satellite crosses both of their zenith positions (which happens once per day). We further assume a worst-case scenario such that the stations only interact with the satellite when the zenith positions are crossed and that both stations assume similar operational conditions.

It is possible to quantify the performance of satellite communications by considering a *daily key rate*, i.e., the number of secret bits that may be shared per day. This allows us to utilize an average orbital rate R_{orb} associated with uplink or downlink operations in daytime or nighttime, representing an average secret-key rate per link usage. Due to the dynamic nature of SQC and the fact that we consider communication with both stations only once per day, this daily rate will be constant with respect to ground-based end-to-end distances. The number of secret bits that can be shared in a zenith-crossing passage is then given by the effective transit time for the quantum communications $t_Q(h)$ as a function of the altitude and a typical clock frequency that we set as $\alpha = 10$ MHz. The average daily rate in a given configuration is thus

$$R_{\text{daily}}^{\text{sat}} \approx \alpha t_Q(h) R_{\text{orb}}^i, \quad (20)$$

for which i identifies whether the rate is associated with the CV-QKD protocol operating in uplink or downlink protocol during daytime or nighttime.

For downlink operations at altitude $h = 530$ km, initial beam spot size $\omega_0 = 40$ cm, and receiver aperture $a_R = 1$ m, these setup parameters lead to the nighttime or daytime rates [26],

$$R_{\text{orb}}^{\text{down}} \approx \begin{cases} 3.066 \times 10^{-2} & \text{bits per use (night),} \\ 3.041 \times 10^{-2} & \text{bits per use (day).} \end{cases} \quad (21)$$

For uplink, we consider an altitude $h = 103$ km and similar setups (but now with a spot size $\omega_0 = 60$ cm and a wider aperture $a_R = 2$ m) leading to the rate

$$R_{\text{orb}}^{\text{up}} \approx \begin{cases} 4.244 \times 10^{-2} & \text{bits per use (night),} \\ 2.737 \times 10^{-2} & \text{bits per use (day).} \end{cases} \quad (22)$$

Note that in both configurations, the daytime and nighttime rates are very similar. This is due to effective noise filtering that can be performed with this kind of CV-QKD protocol. Such protocols are able to realistically exploit CV quantum systems and interferometric measurements in order to achieve much narrower frequency filters than is possible with discrete variable (DV) protocols (for more details, see Ref. [26]). As a result, the increased background thermal noise experienced at the receiver in day time does not cause the rate to deteriorate significantly.

C. Comparison with ground-based networks

As we have established in previous sections, end-to-end distance independence is a critical design feature for the construction of effective quantum networks. It is a feature that can be achieved provided that one carefully monitors the link length, the nodal density, and the limits of the quantum communication rates. Yet, as shown in the previous section, it can be very resource intensive and costly to promise strong end-to-end rates between long-distance end users if we choose to solely utilize ground-based fiber networks. For this reason, it is important to understand the limits of large-scale quantum networks for long-range communication. Moreover, it is invaluable to determine when SQC may be superior and offer a feasible cost-efficient route to global quantum communication.

Determination of *when* SQC is advantageous requires a strict quantitative comparison with ground-based fiber networks. In this section, we aim to benchmark the optimal performance of global quantum fiber networks against practical near-term SQC capabilities. More precisely, we compare daily secret key rates obtained between globally distant end users via:

- (i) A global-scale (k, Λ) -WR fiber network with capacity-achieving links.
- (ii) A single sun-synchronous satellite operating at the achievable rates given in Eqs. (20)–(22), using realistic devices and the practical CV-QKD protocol discussed in Sec. IV B.

Clearly, the resources accessed by an ideal (k, Λ) -WR fiber network are significantly greater than the single satellite and a fairer comparison would be to consider a constellation of satellites—but that is the point. If a single sun-synchronous satellite, operating at realistic rates, is able to outperform a global fiber network within a meaningful resource regime, this offers clear evidence for the superiority (and necessity) of SQC for global quantum communications. Using the tools developed throughout this paper, our comparison can be carried out expediently and analytically.

Assume two globally distant end users, Alice and Bob. We need not consider a specific end-to-end distance, since the (k, Λ) WRNs are end-to-end-distance independent. By considering a daily key rate and the operational setup explained in Sec. IV B, SQC is also end-to-end-distance independent. We are left to compute the daily capacity of the WR fiber network. We consider that the fiber network operates constantly for a day using capacity-achieving links with maximum link length $d_{\mathcal{N}}^{\max}$. Given $t_{\text{daily}} = 8.64 \times 10^4$ s as the number of seconds in a day and again assuming $\alpha = 10$ MHz, it can be shown that the average number of secret-key bits per day satisfies

$$R_{\text{daily}}^{(k, \Lambda)}(d_{\mathcal{N}}^{\max}) \lesssim -\frac{\alpha t_{\text{daily}}}{\delta} \log_2(1 - 10^{-\gamma d_{\mathcal{N}}^{\max}}), \quad (23)$$

where δ is defined in Eq. (11). Repeater chains can be considered in a similar manner. The repeater-chain capacity is equal to the single-edge capacity associated with the longest internodal separation in the chain. Hence, the average daily secret-key rate of a repeater chain is [19]

$$R_{\text{daily}}^{\text{chain}}(d_{\mathcal{N}}^{\max}) \lesssim -\alpha t_{\text{daily}} \log_2(1 - 10^{-\gamma d_{\mathcal{N}}^{\max}}). \quad (24)$$

In order to perform a quantitative comparison between satellite and ground-based quantum communications, we can compute the log ratio between their daily rates,

$$\Delta K_{\text{daily}} := 10 \log_{10} \left(\frac{R_{\text{daily}}^{(k, \Lambda)}}{R_{\text{daily}}^{\text{sat}}} \right), \quad (25)$$

which determines a *daily-rate advantage* in decibels (dB). An analogous quantity can be derived for the repeater chain. By studying the daily-rate advantage as a function of the maximum internodal separation and the nodal density, we can then determine conditions for which SQC begins to outperform the global ground-based networks. That is,

$$\begin{aligned} \Delta K_{\text{daily}} > 0 &\implies \text{fiber-network advantage,} \\ \Delta K_{\text{daily}} = 0 &\implies \text{equal performance,} \\ \Delta K_{\text{daily}} < 0 &\implies \text{satellite advantage.} \end{aligned} \quad (26)$$

Hence, there exists a critical internodal separation $d_{\mathcal{N}}^*$ and a critical nodal density $\rho_{\mathcal{N}}^*$ for which $\Delta K_{\text{daily}} = 0$.

Beyond $d_{\mathcal{N}}^*$ or below $\rho_{\mathcal{N}}^*$, a single sun-synchronous satellite quantum repeater is more effective than a global fiber network.

Figure 3 illustrates results for the daily-rate advantage over SQC for a repeater chain and a number of quantum WRNs with various connectivity properties. In particular, we compare the resource demands of SQC with $k = 6, 8,$ and 16 WRNs based on the network cells shown in Fig. 2(a). Each architecture will possess its own unique critical values, defining a limiting property of the network. This comparison involves the consideration of a number of SQC operational setups and conditions, which are summarized in Fig. 3; regarding the time of operation (night or day), the physical direction of communication (uplink or downlink), the satellite altitude, the initial beam spot size, and the receiver-aperture radius. It is important to note that we can *always* exploit the superior communication direction (downlink) for the purposes of QKD between end users, due to the independence of physical and logical flow (as discussed in Sec. II). Therefore, the critical properties $\rho_{\mathcal{N}}^*$ and $d_{\mathcal{N}}^*$ are computed as the values for which $\Delta K_{\text{daily}} = 0$ with respect to SQC downlink rates.

In Figs. 3(a)–3(c), we plot the maximum tolerable fiber length permitted in a repeater chain and each WRN required to guarantee ΔK_{daily} advantage over the single-satellite repeater. The critical fiber length for a quantum repeater chain operating at the ultimate limit is $d_{\text{rep}}^* \approx 215$ km, which offers a lower bound on repeater-assisted ground-based strategies. This can be extended by quantum networks using multipath routing strategies, as WRNs are able to tolerate longer lossy channels at the expense of greater resource demands. This is clear from the results in Fig. 3, where extending the critical separation by approximately 100 km requires a $k = 16$ regular network, for which $d_{\mathcal{N}}^* \approx 320$ km.

We may also identify the minimum required WRN nodal density, $\rho_{\mathcal{N}}^*$, for obtaining ground-based advantage over a single satellite, plotted in Figs. 3(d)–3(f). Analysis of this property provides an appreciation of the resources demanded by these fiber networks. As similarly identified in Sec. III D, while the WRNs with lower regularity are constrained to shorter link lengths, the required nodal density at poorer end-to-end rates (low levels of advantage) is smaller than that of better-connected designs. We find that the critical nodal densities $\rho_{\mathcal{N}}^*$ are of order 10^{-5} nodes per km^2 ; e.g., for $k = 6$ we find that $\rho_{\mathcal{N}}^* \approx 1.49 \times 10^{-5}$; for $k = 16$ we gather $\rho_{\mathcal{N}}^* \approx 5.84 \times 10^{-5}$; etc.

These are expensive values when put into the perspective of a global communication scenario. Let us take a naive scenario from a practical point of view, but one that is informative nonetheless. Consider quantum communication between distant end users located in remote cities across continental Europe (e.g., Paris to Moscow) whose land surface area spans approximately $A \approx 1 \times 10^7$ km^2 . In terms of truly global communications, this is relatively

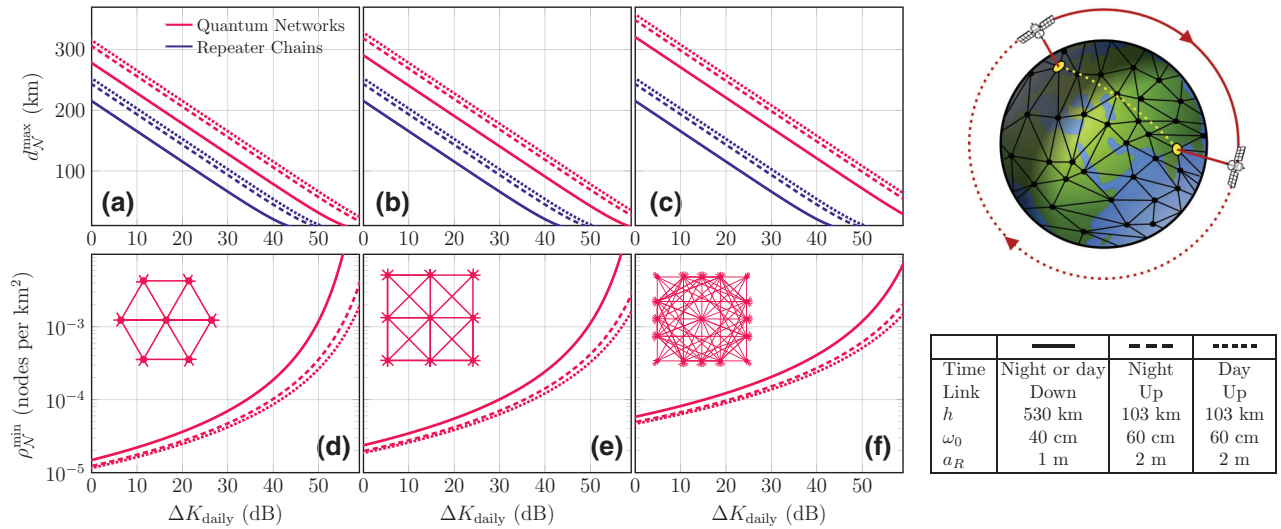


FIG. 3. The daily secret-key-rate advantage ΔK_{daily} in Eq. (25) achieved by fiber-based quantum WRNs and repeater chains with capacity-achieving links over a single sun-synchronous satellite-based repeater operating at practical achievable rates from Eqs. (21) and (22). The architecture of each WRN is shown in the insets to (d)–(f), such that vertically aligned panels use the same architecture. (a)–(c) Plots of ΔK_{daily} with respect to the maximum fiber length permitted within each structure, $d_{\mathcal{N}}^{\text{max}}$. (d)–(f) Plots of the relationship between the daily rate advantage ΔK_{daily} and the minimum nodal density required in each WRN to achieve it. Satellite-based advantage can be achieved when $\Delta K_{\text{daily}} \leq 0$. All considered satellite setup parameters are shown in the legend describing the operation time, direction, altitude h , spot size ω_0 , and receiver aperture a_R .

local. We can choose to communicate between remote cities using a satellite in orbit acting as a dynamic quantum repeater. Alternatively, we can construct a quantum fiber network across the continent. In this scenario, for an ideal $k = 6$ WR quantum fiber network operating at its ultimate flooding capacity to simply match the already achievable daily rate of a single sun-synchronous satellite would require at least $n \geq A\rho_{\mathcal{N}}^* \approx 150$ repeater stations operating constantly for 24 h. Clearly, a network of this form operating at realistic rates, under stricter physical conditions (considering thermal noise), would demand even greater resources.

While the classical Internet can exploit fiber-optic links that are thousands of kilometers long, a fiber-based quantum Internet is severely limited by short link lengths, resulting in remarkably costly resources for tasks that are already within reach of SQC. These results strongly suggest that a future quantum Internet will benefit significantly from the use of SQC and will be integral to the construction of global quantum communication networks.

V. CONCLUSIONS

In this work, we investigate the optimal performance of global quantum communication networks to characterize the ultimate limits of a fiber-based quantum Internet. This analysis is based on an underlying network architecture that exploits weak regularity to construct powerful highly connected networks. Crucially, these bounds

allow us to benchmark the performance of a global quantum network versus that of a single sun-synchronous satellite acting as a dynamic repeater. The result of this comparison emphasizes the power of SQC and the vast network resources that are required to outperform a single satellite in orbit at global distances. These findings strongly motivate the utilization of ground-satellite connections within large-scale quantum networks. It is clear that free-space ground-satellite links will be integral to long-range quantum communications, as their cooperation with ground-based infrastructure as dynamic repeaters will be invaluable.

This work introduces useful analytical techniques for the study of ideal quantum networks that can be readily employed for future investigative paths. Indeed, the study of hybrid fiber and/or satellite networks is a topic of immediate interest, exploiting the power of SQC to enhance (rather than compete with) ground-based networks. Furthermore, the expansion of these methods to incorporate multiple satellites introduces the possibility of highly transmissive satellite-satellite channels at high altitudes.

ACKNOWLEDGMENTS

C.H acknowledges funding from the EPSRC via a Doctoral Training Partnership (EP/R513386/1). S.P acknowledges funding by the European Union via ‘‘Continuous Variable Quantum Communications’’ (CiViQ, Grant Agreement No. 820466).

- [1] M. A. Nielsen and I. L. Chuang, *Quantum Computation and Quantum Information: 10th Anniversary Edition* (Cambridge University Press, USA, 2011), 10th ed.
- [2] J. Watrous, *The Theory of Quantum Information* (Cambridge University Press, Cambridge, 2018).
- [3] A. S. Holevo, *Quantum Systems, Channels, Information* (De Gruyter, Berlin-Boston, 2019).
- [4] F. Arute, K. Arya, R. Babbush, D. Bacon, J. C. Bardin, R. Barends, R. Biswas, S. Boixo, F. G. S. L. Brandao, and D. A. Buell *et al.*, Quantum supremacy using a programmable superconducting processor, *Nature* **574**, 505 (2019).
- [5] H. J. Kimble, The quantum Internet, *Nature* **453**, 1023 (2008).
- [6] S. Pirandola and S. L. Braunstein, Physics: Unite to build a quantum Internet, *Nature* **532**, 169 (2016).
- [7] M. Razavi, *An Introduction to Quantum Communications Networks* (Morgan & Claypool Publishers, 2018), p. 2053.
- [8] S. Pirandola, U. L. Andersen, L. Banchi, M. Berta, D. Bunandar, R. Colbeck, D. Englund, T. Gehring, C. Lupo, and C. Ottaviani *et al.*, Advances in quantum cryptography, *Adv. Opt. Photonics* **12**, 1012 (2020).
- [9] A. Serafini, *Quantum Continuous Variables: A Primer of Theoretical Methods* (CRC Press, Taylor & Francis Group, Boca Raton, FL, 2017).
- [10] C. Weedbrook, S. Pirandola, R. García-Patrón, N. J. Cerf, T. C. Ralph, J. H. Shapiro, and S. Lloyd, Gaussian quantum information, *Rev. Mod. Phys.* **84**, 621 (2012).
- [11] S. L. Braunstein and P. van Loock, Quantum information with continuous variables, *Rev. Mod. Phys.* **77**, 513 (2005).
- [12] T. C. Ralph, Continuous variable quantum cryptography, *Phys. Rev. A* **61**, 010303(R) (1999).
- [13] S. Pirandola, R. Laurenza, C. Ottaviani, and L. Banchi, Fundamental limits of repeaterless quantum communications, *Nat. Commun.* **8**, 15043 (2017).
- [14] S. Pirandola, R. García-Patrón, S. L. Braunstein, and S. Lloyd, Direct and Reverse Secret-Key Capacities of a Quantum Channel, *Phys. Rev. Lett.* **102**, 050503 (2009).
- [15] P. Slepian, *Mathematical Foundations of Network Analysis* (Springer-Verlag, New York, 1968).
- [16] T. M. Cover and J. A. Thomas, *Elements of Information Theory* (Wiley, New Jersey, 2006).
- [17] A. S. Tanenbaum and D. J. Wetherall, *Computer Networks* (Pearson, 2010), 5th ed.
- [18] A. El Gamal and Y.-H. Kim, *Network Information Theory* (Cambridge University Press, Cambridge, 2011).
- [19] S. Pirandola, End-to-end capacities of a quantum communication network, *Commun. Phys.* **2**, 51 (2019).
- [20] J. Biamonte, M. Faccin, and M. De Domenico, Complex networks from classical to quantum, *Commun. Phys.* **2**, 53 (2019).
- [21] S. Brito, A. Canabarro, R. Chaves, and D. Cavalcanti, Statistical Properties of the Quantum Internet, *Phys. Rev. Lett.* **124**, 210501 (2020).
- [22] Q. Zhuang and B. Zhang, Quantum communication capacity transition of complex quantum networks, *Phys. Rev. A* **104**, 022608 (2021).
- [23] B. Zhang and Q. Zhuang, Quantum Internet under random breakdowns and intentional attacks, *Quantum Sci. Technol.* **6**, 045007 (2021).
- [24] S. Pirandola, Limits and security of free-space quantum communications, *Phys. Rev. Res.* **3**, 013279 (2021).
- [25] J. S. Sidhu, S. K. Joshi, M. Gündoğan, T. Brougham, D. Lowndes, L. Mazzarella, M. Krutzik, S. Mohapatra, D. Dequal, and G. Vallone *et al.*, Advances in space quantum communications, *IET Quant. Comm.* **2**, 182 (2021).
- [26] S. Pirandola, Satellite quantum communications: Fundamental bounds and practical security, *Phys. Rev. Res.* **3**, 023130 (2021).
- [27] J. Yin, Y. Cao, Y.-H. Li, S.-K. Liao, L. Zhang, J.-G. Ren, W.-Q. Cai, W.-Y. Liu, B. Li, H. Dai, and G.-B. Li *et al.*, Satellite-based entanglement distribution over 1200 kilometers, *Science* **356**, 1140 (2017).
- [28] J.-G. Ren, P. Xu, H.-L. Yong, L. Zhang, S.-K. Liao, J. Yin, W.-Y. Liu, W.-Q. Cai, M. Yang, and L. Li *et al.*, Ground-to-satellite quantum teleportation, *Nature* **549**, 70 (2017).
- [29] S.-K. Liao, J. Lin, J. Ren, W. Liu, J. Qiang, J. Yin, Y. Li, Q. Shen, L. Zhang, and Y. Cao *et al.*, Space-to-ground quantum key distribution using a small-sized payload on Tiangong-2 space lab, *Chin. Phys. Lett.* **34**, 090302 (2017).
- [30] A. Villar, A. Lohrmann, X. Bai, T. Vergoossen, R. Bedington, C. Perumangatt, H. Lim, T. Islam, A. Reezwana, and Z. Tang *et al.*, Entanglement demonstration on board a nano-satellite, *Optica* **7**, 734 (2020).
- [31] J. Yin, Y.-H. Li, S.-K. Liao, M. Yang, Y. Cao, L. Zhang, J.-G. Ren, W.-Q. Cai, W.-Y. Liu, S.-L. Li, and R. Shu *et al.*, Entanglement-based secure quantum cryptography over 1,120 kilometres, *Nature* **582**, 501 (2020).
- [32] R. Wilson, *Introduction to Graph Theory* (Longman, Essex, 1996), 4th ed.
- [33] L. R. Ford and D. R. Fulkerson, Maximal flow through a network, *Can. J. Math.* **8**, 399 (1956).
- [34] J. Edmonds and R. M. Karp, Theoretical improvements in algorithmic efficiency for network flow problems, *J. ACM* **19**, 248 (1972).
- [35] J. B. Orlin, in *Proceedings of the forty-fifth annual ACM symposium on Theory of computing, STOC'13* (2013), p. 765.
- [36] B. Waxman, Routing of multipoint connections, *IEEE J. Sel. Areas Commun.* **6**, 1617 (1988).
- [37] See the Supplemental Material at <http://link.aps.org/supplemental/10.1103/PRXQuantum.3.010349> for definitions, lemmas, theorems, and their proofs for theoretical developments discussed in the main text.